AIP | Applied Physics Letters

Field effect modulated nanofluidic diode membrane based on Al2O3/W heterogeneous nanopore arrays

Songmei Wu, Fabien Wildhaber, Arnaud Bertsch, Juergen Brugger, and Philippe Renaud

Citation: Appl. Phys. Lett. **102**, 213108 (2013); doi: 10.1063/1.4807781
View online: http://dx.doi.org/10.1063/1.4807781
View Table of Contents: http://apl.aip.org/resource/1/APPLAB/v102/i21
Published by the American Institute of Physics.

Field effect modulated nanofluidic diode membrane based on Al_2O_3/W heterogeneous nanopore arrays

Songmei Wu,[a] Fabien Wildhaber, Arnaud Bertsch, Juergen Brugger, and Philippe Renaud
Microsystems Laboratory, École Polytechnique Fédérale de Lausanne, EPFL STI-IMT-LMIS, Station 17, 1015 Lausanne, Switzerland

(Received 18 April 2013; accepted 5 May 2013; published online 29 May 2013)

We developed Al_2O_3/W heterogeneous nanopore arrays for field effect modulated nanofluidic diodes. They are fabricated by transferring self-organized nanopores of anodic aluminium oxide into a W thin film. The nanopores are ~20 nm in diameter and 400 nm in length. After mild oxidation, approximately 10 nm WO_3 grows on the surface of W, forming a conformal and dense dielectric layer. It allows the application of an electrical field through the surrounding W electrode to modulate the ionic transport across the entire membrane. Our experimental findings have potential applications in high throughput controlled delivery and electrostatic sorting of biomolecules. © *2013 AIP Publishing LLC*. [http://dx.doi.org/10.1063/1.4807781]

A nanofluidic diode possesses the unique property of creating ionic current rectification in nanochannels.[1–5] It is a basic element for directional control of ionic and molecular transport mimicking biological ion channels.[6] Various approaches have been developed to achieve asymmetric transport in a nanochannel. A typical nanofluidic diode consists of heterogeneous surface charges along a nanochannel by using surface functionalization or different native oxides.[7–11] Alternatively, for a mono-charged nanochannel, the breaking of symmetry is possible through geometry,[12] gradient in ion concentration[13] or liquid viscosity,[14] and external chemical stimuli such as pH[15] and binding of polyvalent cations.[16] However, the property of the diode cannot be modified once it is made without changing its chemical environment.

Tuning the rectifying property of a nanofluidic diode *in situ* through an external electrode is important for controlled delivery, electrostatic sorting, and detection in biochemical processes.[17–19] A gate electrode can be used to modulate the potential and charge density of the electrical double layer near the channel walls in electrolytes. Several types of planar nanofluidic diodes were fabricated based on conventional "etching followed by bonding" technique.[7,10,13] In such a configuration a top gate electrode is used to modulate ionic transport through the nanochannels for nanofluidic transistors.[20–23] However, planar nanochannels are generally long with small cross section and therefore have very small throughput of ionic current.

We present here a membrane approach for field effect modulated nanofluidic diodes based on nanopore arrays. The obvious advantage of a membrane is that it presents a high number of parallel short nanopores within a small area. Figure 1(a) shows the schematic geometry of the membrane. The nanopore is composed of heterogeneous Al_2O_3 and W layers. The surface of the W metal is passivated by WO_3 dielectric thin film via thermal oxidation. Figure 1(b) illustrates the working principle of a field effect reconfigurable nanofluidic diode. It is a three-terminal device. A pair of Ag/AgCl electrodes is used to apply bias and measure ionic conductance across the membrane. The gate potential is applied on the W layer. The current through drain (I_D) and gate (I_G) are monitored simultaneously. The gate potential regulates the charge polarity and density of the electrical double layer both inside the nanochannel and on the surface of the membrane at the W side. Consequently, the rectification property of the membrane can be modulated by the gate potential.

We have developed a strategy to fabricate heterostructured nanopore membranes based on pattern transfer of anodic aluminium oxide (AAO).[24] The process is described in Figure S1 of the supplemental material.[25] Briefly, 200 nm W was deposited on a freestanding low stress SiN membrane followed by an annealing process (Figure S2 in the supplemental material[25]). Afterwards, 150 nm Al was deposited and

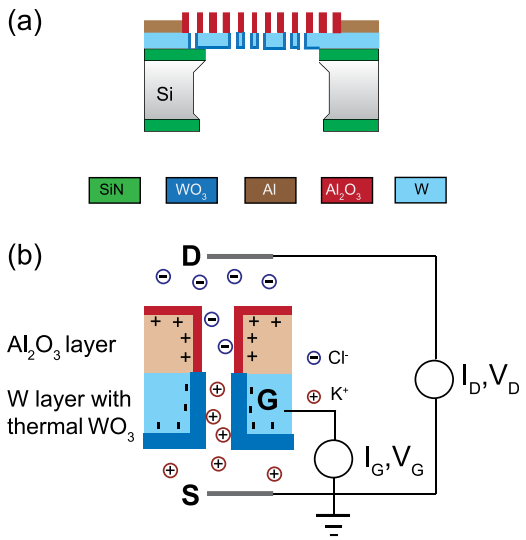

FIG. 1. Schematics of (a) an Al_2O_3/W heterogeneous nanopore membrane. The surface of W is passivated by thermally grown WO_3; (b) working principle as a field effect modulated nanofluidic diode. A pair of Ag/AgCl electrodes is used to apply bias and measure ionic current across the membrane in electrolytes. The gate potential regulates the charge density of the electrical double layer at the W side. As the result, the rectification property of the entire device can be modulated through the change of asymmetry in charge polarities and densities within the nanopores.

[a]Author to whom correspondence should be addressed. Electronic mail: songmei.wu@epfl.ch

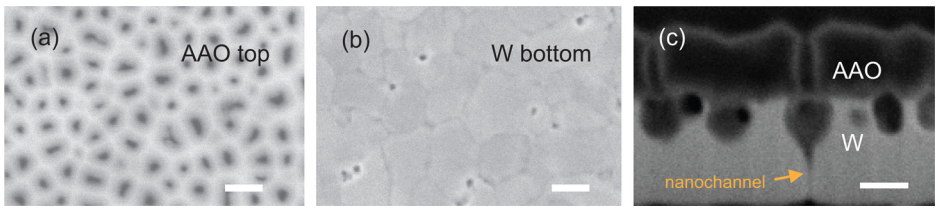

FIG. 2. SEM images of (a) alumina top, (b) W bottom, and (c) FIB-SEM image of cross sections of heterogeneous Al_2O_3/W nanopore membrane (scale bar 100 nm). The pore size of the top alumina is 26 ± 7 nm. The openings in the W layer are smaller (<20 nm) and mostly located at grain boundaries. The pore density of ~20 pores μm^{-2} in the W bottom is relatively low, compared to ~200 pores μm^{-2} of the top alumina layer. W etching process through top alumina creates nanocavities with nanochannels open through the membrane.

anodized to create self-organized alumina nanopores. By reactive ion etching of W through AAO, some of the top nanopores penetrate into the bottom W layer. Finally the membrane was released by selective etching of the supporting SiN layer. The nanopores are thus composed of Al_2O_3 layer and W layer with natively positive and negative surface charges, respectively. A conformal dielectric layer is formed at W surface by mild oxidation.

The SEM sample characterizations are shown in Figure 2. Figure 2(a) reveals typical dense alumina nanopore pattern generated by anodization of a thin Al film. It shows a distribution in pore size and shape. The pore size of the top alumina layer is 26 ± 7 nm. The openings in the W layer (Figure 2(b)) are smaller (<20 nm) and mostly located at grain boundaries. The pore density of ~20 pores μm^{-2} in the W bottom is relatively low, compared to ~200 pores μm^{-2} of top AAO layer. This means that only 10% of AAO pores are fully transferred through W. The profile of the hetero-structured nanopore is shown in the FIB-SEM cross section image Figure 2(c). The structure was formed after 2 min of SF_6 reactive ion etching of W by using AAO as local mask. The AAO layer becomes ~30 nm thinner but keeps similar pore size and vertical pore shape. In comparison, the nanochannels in the W layer are very different. There are plenty of nanocavities formed at the interface of alumina and W layer by SF_6 plasma etching, where the fluorine radicals can attach to the W sidewall and cause isotropic undercutting.[26,27] During the etching process, some of the cavities eventually open to the bottom of W, preferentially at the grain boundaries, forming funnel shaped channels for ion transport. The average diameter of the obtained nanochannels is in the range of 10–20 nm.

Subsequently we use mild thermal oxidation to grow a conformal dielectric thin film selectively on the W surface. Among two stable tungsten oxides of WO_2 and WO_3, WO_3 is the most thermodynamically stable oxide at low temperature and atmospheric pressure. Thermal oxidation of W films is strongly dependent on the temperature with a marked increase in oxidation rate at temperatures above 300 °C.[28,29] However, high temperature oxidation (>600 °C) often produces cracks due to the high stress between WO_3 and W.[30] After thermal oxidation at 350 °C for 2 h, the top alumina layer remains unchanged but ~10 nm of tungsten oxide can be clearly seen on the surface of the nanocavities. The tungsten oxide shrinks the size of nanocavities but does not clog the nanochannel, presumably due to slow oxidation rate as the result of small volume for oxygen diffusion.

Prior to thermal oxidation, ion transport properties of native membranes were characterized in KCl electrolyte at varied concentrations ranging from 0.1 mM to 1 M. Clear rectifying behavior appeared from 0.1 mM to 0.1 M electrolytes as summarized in Figure S3 of the supplemental material.[25] This is expected because the native oxide surface on W possesses negatively charged surfaces as suggested by its point of zero charge (PZC) value that is less than 0.5,[31] while PZC for positively charged Al_2O_3 is 8.[10]

We now focus on the study of field effect modulated ion transport in 1 mM KCl solution. It was performed by measuring the IV curves across the membrane under different gate potentials applied on the embedded W electrode. For a three-terminal device, it is important to have a high strength gate dielectric to diminish the effect of leakage current especially in electrolyte environment. The measured gate leakage current I_G is below the detection level of the amplifier ($I_G < 1$ nA) within the gating range of −0.5 V–0.5 V, making no disturbance on measured value of drain current I_D. Tungsten oxide has high-κ dielectric constant ε_r, varying from 20 to 300, depending on the preparation method. The conformal and dense dielectric layer induced by mild oxidation allows the application of efficient gating at low potentials through a thin dielectric. Generally, the dielectric strength of a gate oxide layer grown by thermal oxidation is stronger than that deposited by atomic layer deposition (ALD). We have tested dielectrics of Al_2O_3 and HfO_2 grown by ALD, with which thin layers below 10 nm breakdown below 0.5 V potential while thicker layers cause clogging of nanopores.

Figure 3(a) plots the IV curves through the membrane under negative gate potentials. It is clearly seen that the

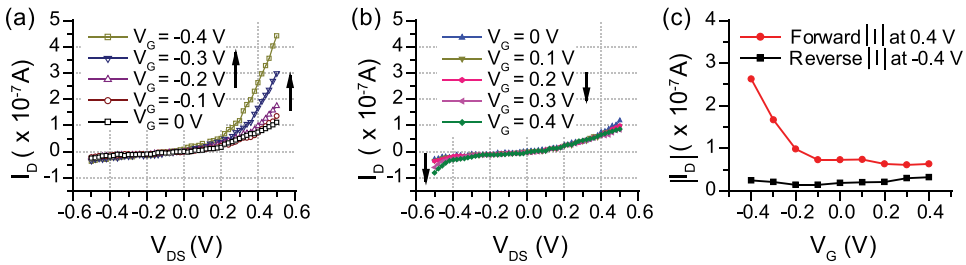

FIG. 3. Ionic transport properties of a field effect modulated diode membrane in 1 mM KCl solution: (a) IV curves under negative gate potentials; (b) IV curves under positive gate potentials; (c) forward and reverse current values at different gate potentials.

forward current increases significantly with gate potential varying from 0 to −0.4 V. While at the same time, the reverse current remains nearly the same. Very differently, the IV curves only weakly depend on positive gate potentials as shown in Figure 3(b). Modulus of forward current values at 0.4 V and reverse current values at −0.4 V under different gate potentials are summarized in Figure 3(c). For the forward current, efficient response to a negative gate potential is the result of electrostatically induced high charge density of the electrical double layer at the W side of the membrane. Low level of control on positive gate potential side reflects the buffering effect by dissociation of hydroxyl groups on the surface of WO_3. The reverse current is rather independent of gate potentials, indicating that it is dominated by the sample geometry or breaking down of water molecules rather than the charge density of the double layer. This is presumably related to the short ionic channels as suggested by simulations.[4,32] The overall effect on rectifying factor taken between $|I_D|$ at 0.4 V and −0.4 V can be modulated from 2 to 11.

The response of regulation on electrical double layer properties through a gate potential for WO_3 can be interpreted by a metal-dielectric-electrolyte electrochemical model. Considering a flat gate electrode in electrolyte as depicted in Figure 4(a), the equivalent circuit consists of two capacitors of gate dielectric ($C_{Dielectric}$) and Stern layer (C_{Stern}) plus Poisson-Boltzmann description of the diffusion layer. If the oxide has zero surface charge, the induced charge density of the electrical double layer (σ_{DL}) is equal to that of the dielectric surface (σ_{DE}): $\sigma_{DL} = \sigma_{DE}$. However, most native oxides spontaneously obtain surface charges on exposure to aqueous solution due to dissociation of hydroxyl groups. The low PZC value (<0.5) of WO_3 indicates a single negatively ionizable oxide surface: $W\text{-}OH \rightleftharpoons W\text{-}O^- + H^+$. The dissociation of surface ionizable groups on oxides tends to shield the electrostatic charges induced by a gate potential: under a negative gate potential, the oxide surface groups are protonated to form hydrates (W-OH). On contrary, more negative charged groups ($W\text{-}O^-$) form under a positive gate potential. The effective charge density of the electrical double layer σ_{DL} is therefore the sum of charge density of the dielectric σ_{DE} and that of dissociated oxide surfaces (σ_{diss}): $\sigma_{DL} = \sigma_{DE} + \sigma_{diss}$. The electrochemical model can be solved analytically based on the dissociation equilibrium under applied gate potentials.[33,34] The results for a typical single negatively charged oxide surface (pK = 7.5, $\varepsilon_r = 20$, $C_{Stern} = 0.2\,C\,m^{-2}$, $d_{DE} = 10\,nm$) in neutral electrolyte (pH = 7) are summarized in Figure 4(b). Γ ($\times 10^{17}\,m^{-2}$) is the total density of ionizable groups at the oxide surface. When $\Gamma = 0$, σ_{DL} is determined only by the dielectric property of the oxide. It is therefore nearly linearly dependent on the

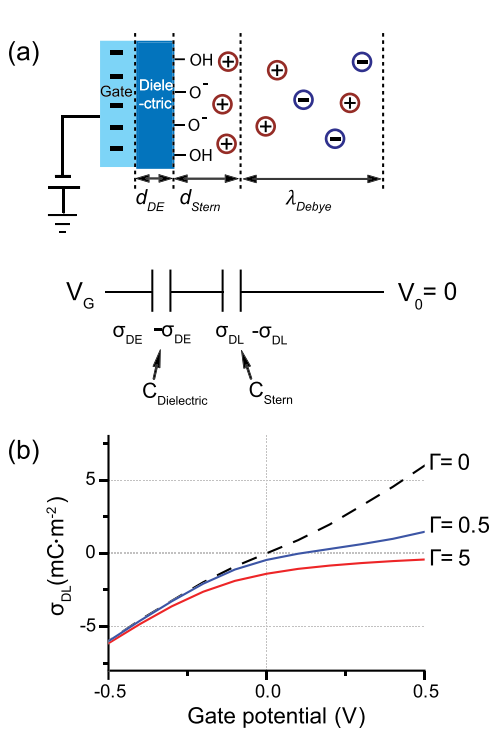

FIG. 4. Electrochemical model of the electrofluidic gating. (a) Schematic of a metal-oxide-electrolyte system and equivalent circuit consists of gate dielectric ($C_{Dielectric}$) and Stern layer (C_{Stern}) plus Poisson-Boltzmann description of the diffusion layer; (b) response of the electrical double layer charge density (σ_{DL}) to applied gate potential for a single negatively charged WO_3 surface ($W\text{-}OH \rightleftharpoons W\text{-}O^- + H^+$, taking pK = 7.5, $\varepsilon_r = 20$, $C_{Stern} = 0.2\,C\,m^{-2}$, $d_{DE} = 10\,nm$) in neutral electrolyte (pH = 7). Γ ($\times 10^{17}\,m^{-2}$) is the total density of ionizable groups at the WO_3 surface. When $\Gamma = 0$, $\sigma_{DL} = \sigma_{DE}$, σ_{DL} is determined only by the dielectric property of the oxide. It is therefore nearly linearly dependent on the gate potential. As for the situations of $\Gamma = 0.5$ and 5, σ_{DL} is much lower at positive gate potentials due to the screening effect of the negative dissociated surface charges ($W\text{-}O^-$) on the oxide.

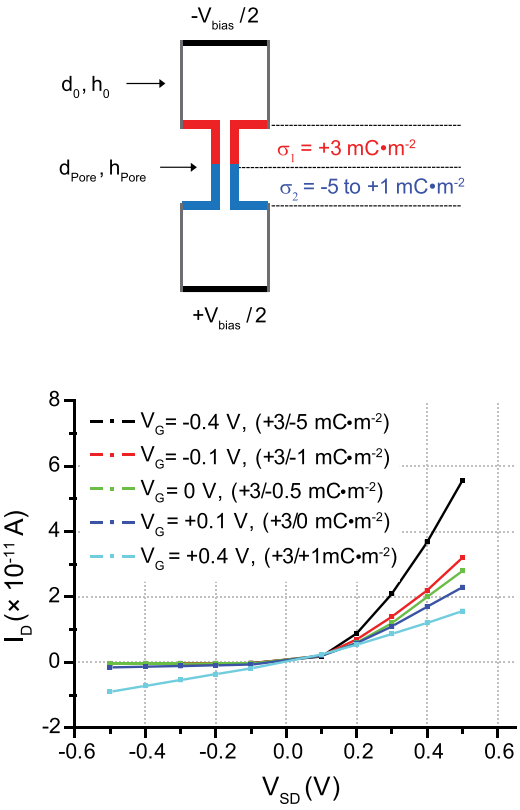

FIG. 5. Ionic transport simulation through a single pore nanofluidic diode based on the Poisson-Nernst-Planck equations. The nanopore is axisymmetric with diameter of 20 nm and total length of 400 nm connected to two bulk reservoirs of 1 mM KCl solution with bias V_{bias}. The heterogeneous nanopore is composed of positive surface charge on the top side (red, $\sigma_1 = +3\,mC\,m^{-2}$) and various surface charge polarities and densities on the down side (blue $\sigma_2 = -5$ to $+1\,mC\,m^{-2}$). The relation between σ_2 and V_G is obtained from the electrochemical model described in Figure 4(b) in the situation of $\Gamma = 0.5 \times 10^{17}\,m^{-2}$.

gate potential. As for the situations of $\Gamma = 0.5$ and 5, σ_{DL} is much lower at positive gate potentials due to the buffering effect of the dissociated negative surface charges.

The modulation of the gate potential on the ionic transport through the membrane can be qualitatively understood by the COMSOL simulation in Figure 5 using the Poisson-Nernst-Planck equations. The model considers a heterogeneous nanopore connected by two reservoirs of 1 mM KCl solution with bias V_{bias}. The nanopore is axisymmetric with diameter of 20 nm and total height of 400 nm. It is composed of a positively charged top side with $\sigma_1 = +3\,\mathrm{mC\,m^{-2}}$ and down side with σ_2 varying from -5 to $+1\,\mathrm{mC\,m^{-2}}$. $\sigma_2 = \sigma_{DL}$ is obtained in Figure 4 at different gate potentials. The same charge polarity and density are also applied to the entrance of corresponding side of nanopores as indicated in the schematic. When the gate potential changes from -0.4 V to $+0.4$ V, the IV curves deviate from ideal rectifying behaviour with lower forward current and higher reverse current. The simulation is qualitatively consistent with the experimental observations shown in Figure 4. The experimental conductance value is about 4 orders of magnitude higher than that of the simulated value for a single pore of 20 nm in diameter, which corresponds to the summed throughput of a pore density of $\sim$20 pores $\mu\mathrm{m}^{-2}$ and a membrane area of $10^4\,\mu\mathrm{m}^2$.

In conclusion, we have demonstrated field effect reconfigurable nanofluidic diode membranes composed of alumina/tungsten (Al_2O_3/W) heterogeneous nanopore arrays. Typical membrane size is $100 \times 100\,\mu\mathrm{m}^2$ with $\sim 10^5$ pores in total. The fabrication process is scalable, based on pattern transfer of self-organized nanopores of anodic aluminium oxide into a W layer. We have provided a simple method to fabricate efficient gate dielectric by thermal oxidation of W at relatively low temperature. The ionic current rectifying behavior through the membrane can be efficiently modulated by an external electrical potential through the W electrode. Our experimental findings have potential applications in controllable molecular separation, chemical processing and biosensing.

The authors would like to gratefully acknowledge the CMI (Center of MicroNanoTechnology) and CIME (Interdisciplinary Center for Electron Microscopy) at EPFL for valuable support of microfabrication processes and FIB-SEM imaging. This work was supported by the EU research project Multiplat (FP7-NMP-2008-SMALL-2), Swiss national foundation project (FNS 200021- 140493) and the Swiss funding nanotera.ch.

[1]H. Daiguji, Y. Oka, and K. Shirono, Nano Lett. **5**, 2274 (2005).
[2]M. E. Gracheva, J. Vidal, and J.-P. Leburton, Nano Lett. **7**, 1717 (2007).
[3]M. E. Gracheva, D. V. Melnikov, and J.-P. Leburton, ACS Nano **2**, 2349 (2008).
[4]I. Vlassiouk, S. Smirnov, and Z. Siwy, ACS Nano **2**, 1589 (2008).
[5]D. V. Melnikov, J.-P. Leburton, and M. E. Gracheva, Nanotechnology **23**, 255501 (2012).
[6]P. L. Smith, T. Baukrowitz, and G. Yellen, Nature **379**, 833 (1996).
[7]R. Karnik, C. Duan, K. Castelino, H. Daiguji, and A. Majumdar, Nano Lett. **7**, 547 (2007).
[8]I. Vlassiouk and Z. S. Siwy, Nano Lett. **7**, 552 (2007).
[9]R. Yan, W. Liang, R. Fan, and P. Yang, Nano Lett. **9**, 3820 (2009).
[10]L.-J. Cheng and L. J. Guo, ACS Nano **3**, 575 (2009).
[11]Y. Lei, W. Wang, W. Wu, and Z. Li, Appl. Phys. Lett. **96**, 263102 (2010).
[12]Z. S. Siwy, Adv. Funct. Mater. **16**, 735 (2006).
[13]L. J. Cheng and L. J. Guo, Nano Lett. **7**, 3165 (2007).
[14]E. C. Yusko, R. An, and M. Mayer, ACS Nano **4**, 477 (2010).
[15]M. Ali, P. Ramirez, S. Mafé, R. Neumann, and W. Ensinger, ACS Nano **3**, 603 (2009).
[16]Y. He, D. Gillespie, D. Boda, I. Vlassiouk, R. S. Eisenberg, and Z. S. Siwy, J. Am. Chem. Soc. **131**, 5194 (2009).
[17]W. Sparreboom, A. van den Berg, and J. C. T. Eijkel, Nat. Nanotechnol. **4**, 713 (2009).
[18]L. Bocquet and E. Charlaix, Chem. Soc. Rev. **39**, 1073 (2010).
[19]A. Piruska, M. Gong, J. V. Sweedler, and P. W. Bohn, Chem. Soc. Rev. **39**, 1060 (2010).
[20]R. Karnik, R. Fan, M. Yue, D. Li, P. Yang, and A. Majumdar, Nano Lett. **5**, 943 (2005).
[21]R. Fan, M. Yue, R. Karnik, A. Majumdar, and P. Yang, Phys. Rev. Lett. **95**, 086607 (2005).
[22]R. Karnik, K. Castelino, and A. Majumdar, Appl. Phys. Lett. **88**, 123114 (2006).
[23]W. Guan, R. Fan, and M. A. Reed, Nat. Commun. **2**, 506 (2011).
[24]S. Wu, F. Wildhaber, O. Vazquez-Mena, A. Bertsch, J. Brugger, and P. Renaud, Nanoscale **4**, 5718 (2012).
[25]See supplementary material at http://dx.doi.org/10.1063/1.4807781 for Figure S1: fabrication process flow of Al_2O_3/W hetero-structured nanopore membranes; Figure S2: stress releasing of a W film on a LS SiN membrane; and Figure S3: ionic transport properties of native diode membranes.
[26]C. W. Jurgensen, R. R. Kola, A. E. Novembre, W. W. Tai, J. Frackoviak, L. E. Trimble, and G. K. Celler, J. Vac. Sci. Technol. B **9**, 3280 (1991).
[27]C. Reyes-Betanzo, S. A. Moshkalyov, A. C. Ramos, J. A. Diniz, and J. W. Swart, J. Electrochem. Soc. **149**, G179 (2002).
[28]A. Warren, A. Nylund, and I. Olefjord, Int. J. Refract. Met. Hard Mater. **14**, 345 (1996).
[29]S. Xu and L. Diao, J. Vac. Sci. Technol. A **26**, 360 (2008).
[30]S. C. Cifuentes, M. A. Monge, and P. Pérez, Corros. Sci. **57**, 114 (2012).
[31]G. A. Parks, Chem. Rev. **65**, 177 (1965).
[32]I. Vlassiouk, S. Smirnov, and Z. Siwy, Nano Lett. **8**, 1978 (2008).
[33]Z. Jiang and D. Stein, Langmuir **26**, 8161 (2010).
[34]Z. Jiang and D. Stein, Phys. Rev. E **83**, 031203 (2011).